

Full Paper

Prediction of rolling resistance coefficient of retreaded truck tyres through numerical simulation

Chukree Daesa and Supasit Rodkwan*

Department of Mechanical Engineering, Faculty of Engineering, Kasetsart University, Bangkok 10900, Thailand

* Corresponding author, e-mail: fengssr@ku.ac.th

Received: 23 May 2017 / Accepted: 18 July 2018 / Published: 10 August 2018

Abstract: Retreaded tyres are commonly used on most highway trucks and buses for economic purposes in the logistics and transportation industry. In the retreading process the tread of worn pneumatic tyres with inspected tyre casing can be effectively remoulded. Nevertheless, an issue of the retreaded truck tyre energy efficiency remains a major challenging task in the industry nowadays. This research aims to obtain an effective simulated tool to determine the rolling resistance coefficient (RRC) of biased pneumatic retreaded truck tyres. In this work a finite element model was developed to predict the RRC for a tyre size of 10.00-20 with three tread patterns using ISO 28580-2009, which specifies methods for measuring the rolling resistance under controlled conditions. The simulated output variables include rolling resistance force, displacement and total strain energy. In addition, laboratory data were obtained through a series of experiments to verify the calculated RRC. The results show that a high degree of correlation between predicted and experimental RRC data can be found. As a result, an RRC prediction model of biased pneumatic retreaded truck tyres developed can effectively be used as a key parameter for fuel consumption improvement on retreaded tyre pattern design in the near future.

Keywords: retreaded truck tyre, rolling resistance coefficient, finite element model, ISO 28580-2009, total strain energy

INTRODUCTION

A retreaded tyre is a worn tyre which is remanufactured through a retreading process. Typically, the precure retreading process consists of an initial visual inspection of the tyre casing for safety issues, a buffing of worn tread, a filling repairing of the tyre surface, a building of a new

precured tread, a curing of the precured tread on the tyre casing, and a final retreaded tyre inspection [1]. The major applications of retreaded tyres are adopted in commercial airplanes, trucks and buses used in the transportation and logistics industry [1]. The benefits resulting from tyre retreading include reduction in transportation cost, recycling of used tyres with positive environmental impact and increase in a value-added product from natural rubber [1]. Various publications related to retreaded tyres have been presented. A mathematical approach based on Bayesian networks was used for decision-making support on tyre retreading [2]. A study of retreaded tyre geographic distribution, tyre replacement market, value-added products in tyre production, retreaded tyre process, and application of used tyres including heat generation, ground rubber, reused direct material, and pyrolysis was carried out to determine the economic status of retreaded tyre remanufacturing [3]. A decision rule model was also developed to obtain the retreading optimisation [3]. A study on the ground mechanical characteristics of retreaded tyres for load vehicles was performed by simulation using ANSYS to describe the failure mechanism of retreaded radial tyres [4]. It is noted that a precured tread has a tread pattern which plays the major role in tyre fuel consumption. Generally, the physical properties of the tread pattern include a tensile strength of 19 MPa or higher, an elongation of 400% or higher, and a hardness of 63-71 Shore A [5].

One of the significant parameters in the tyre industry directly related to vehicle fuel consumption is the tyre rolling resistance (RR). RR is referred to as the energy loss or consumed energy at a specified distance travelled and can be treated as the resisting force when a body rolls on any surface as shown in Figure 1. Hysteresis is considered as the main cause of the tyre RR. In the case of deformable and viscoelastic materials like rubber, hysteretic behaviour such as energy loss in the form of heat exists as a tyre rotates and experiences repeated cycles of the deformation phase such as compression, bending and shearing during the recovery phase. In general the rolling resistance coefficient (RRC), a dimensionless parameter, is referred to as a key variable that exhibits the tyre RR characteristics as stated in ISO 28580-2009 [6], which specifies methods for measuring RR under controlled conditions.

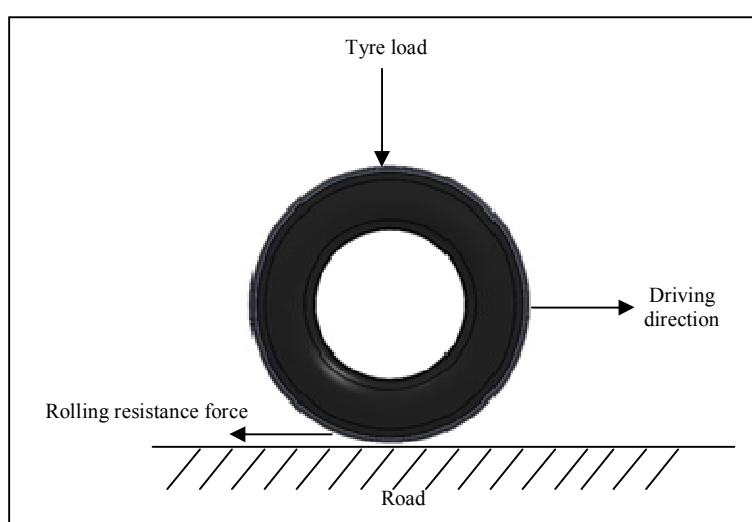


Figure 1. Schematic of the RR on a tyre

A number of selected papers related to the numerical modelling of RR are reviewed in this research work. The RR force and temperature distribution were numerically investigated through the hyperelastic loss on a radial tyre with a specific tread pattern. Nanocomposite materials were introduced and then found to effectively reduce the RR force [7]. The effect of the nanocomposite on RR on a radial tyre was also numerically studied, and substantial improvement in lowering RR was found [8]. The sensitivity coefficient related to fuel consumption and tyre RR was measured according to ISO 28580-2009 to predict the impact of the tyre choice on different vehicle sizes [9]. An experimental verification of the formula conversion of RR from the surface curvature into the corresponding planes was successfully conducted [10]. A study of the effect of tread depth on RR of radial truck tyres was carried out. A higher RR was found as tread depth increased [11]. A higher inflation pressure and a decreasing vertical load result in a lower RR force for a radial ply tyre [12]. An analytical function for the minimum RR considering only the term of material deformation in the energy loss was established for a radial tyre [13]. Using numerical analysis to obtain the stress, strain and RR force in a radial truck tyre, it was found that the rubber tread plays the most important role in the reduction of the RRC to achieve less fuel consumption for vehicles [14]. A static finite element analysis has been developed based on energy dissipation in the homogenisation method using incompressible hyperelastic material assumption to represent the RRC of radial tyres used for passenger cars [15].

There are very limited research investigating the subject of tyre RR of pneumatic retreaded tyres. The tyre model development and tread pattern production of newly manufactured and retreaded tyres rather differ, resulting in different tyre component modelling techniques. In addition, in terms of simulation of the RRC determination, most previous work was only done through hysteresis loss and physical characterisation without consideration of the geometry of tread pattern. Also, there seems to be no work performed on the application of finite element analysis (FEA) simulation to the determination of the RRC of retreaded tyres using recently and globally applied ISO standards. Consequently, in this research a prediction of the RRC of biased pneumatic retreaded truck tyres with different tread patterns through numerical simulation is performed under the conditions of ISO 28580-2009 [6]. Additional work is also experimentally conducted to verify the RRC correlation.

MATERIALS AND METHODS

Biased pneumatic retreaded truck tyres of size 10.00-20 were used in this study. There were of different tread patterns primarily made of natural rubber compound, tyre casing, bias ply and bead. An overall procedure of this research is summarised in Figure 2. Both the numerical simulation and experimental work were carried out to determine the RR force. Subsequently, the force can be used to determine the RRC through a prediction model of the biased retreaded pneumatic truck tyres as well as ISO 28580-2009, which regulates methods for measuring the RR using specified conditions and a determination guideline for the RRC [6].

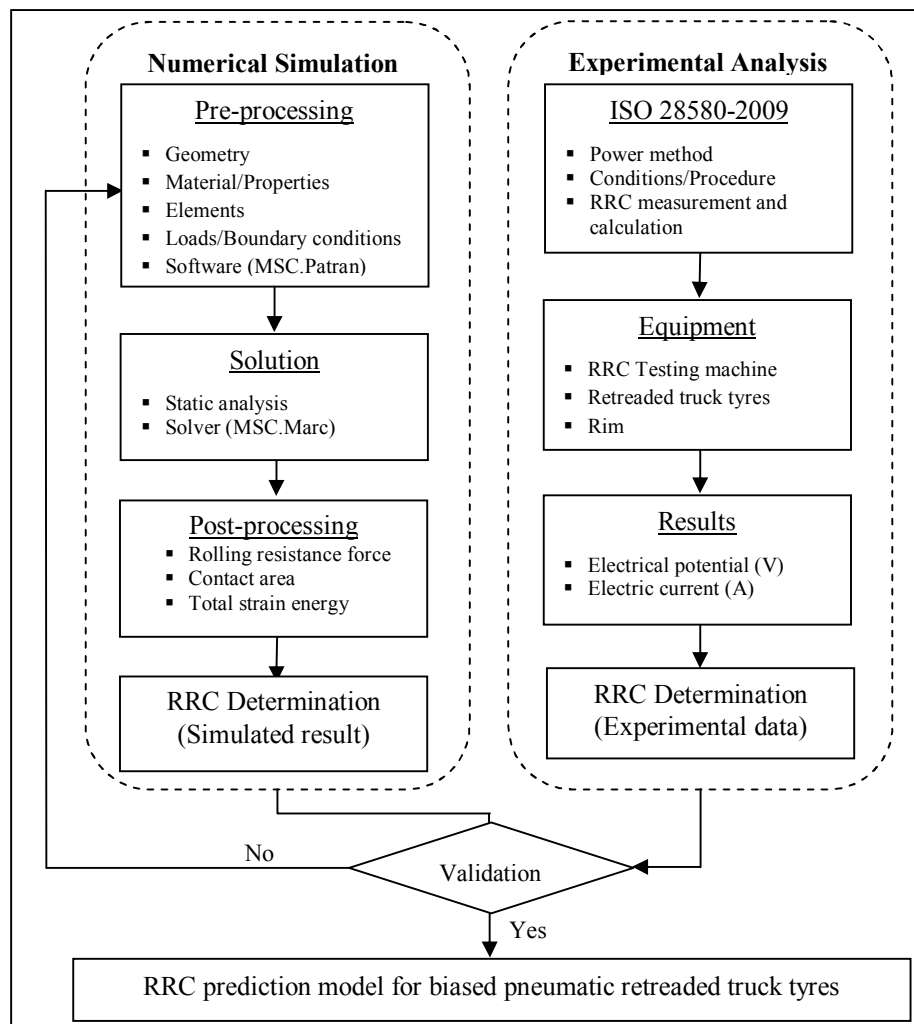


Figure 2. Overall procedure of RRC prediction model development for biased pneumatic retreaded truck tyres

NUMERICAL SIMULATION

Tyre Model

The main components of a biased pneumatic retreaded truck tyre of size 10.00-20, such as tyre size, tread pattern and tyre casing, are shown in Figure 3. The tyre has a 10-inch width and a rim diameter of 20 inches. The rubber tread produces traction on the road surface and a moving force when the tyre rolls. In addition the tread pattern provides a water flow through its grooves on a wet surface and also protects against mechanical damage to the tread itself. Sipes found in some tread patterns reduce heat generated on the tyre. The tread is attached to the tyre casing, the main body of a tyre. The casing is important for keeping the tyre shape and maintaining proper inflation tyre pressure and weight during the rolling stage. The bias ply gives more stiffness to and protection for the tyre casing. The bead is a tyre edge sitting on the wheel and when a tyre is inflated with required pressure, the bead is kept in the groove [16]. Three retreaded truck tyre models for simulation, viz. BSD-1, BSD-2 and BSD-3, are shown in Figure 4.

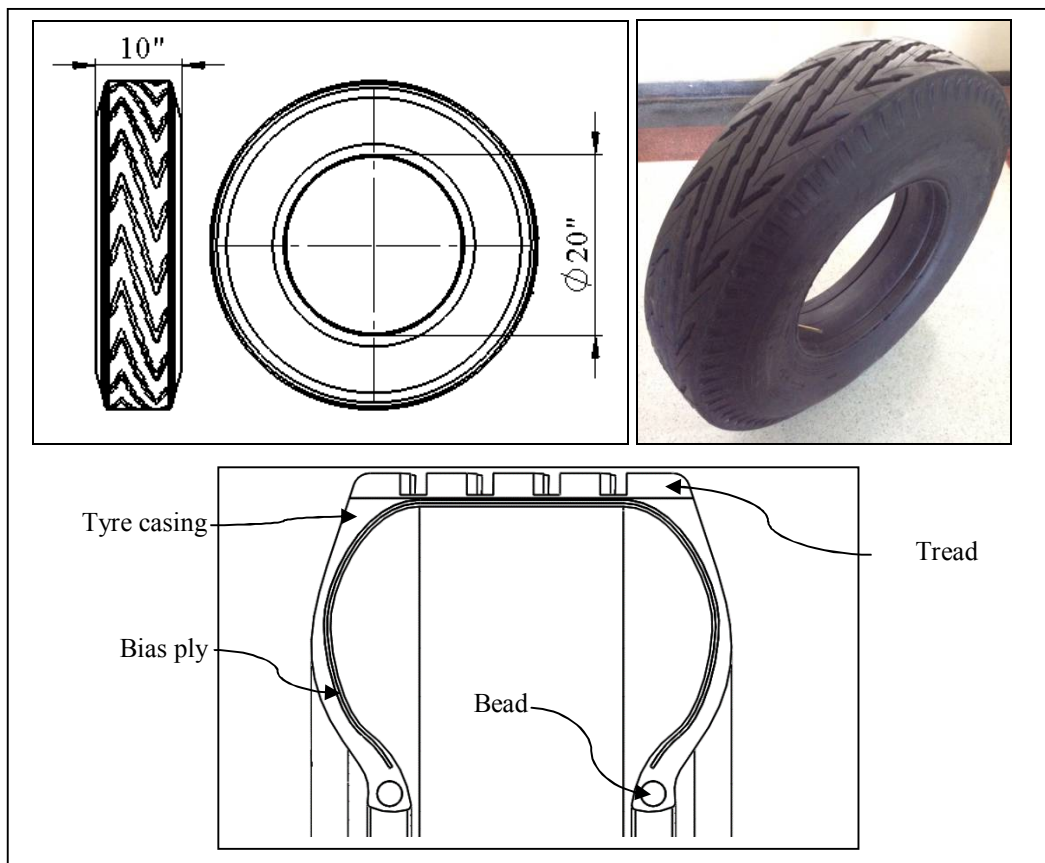


Figure 3. Main components of biased pneumatic retreaded truck tyre of size of 10.00-20

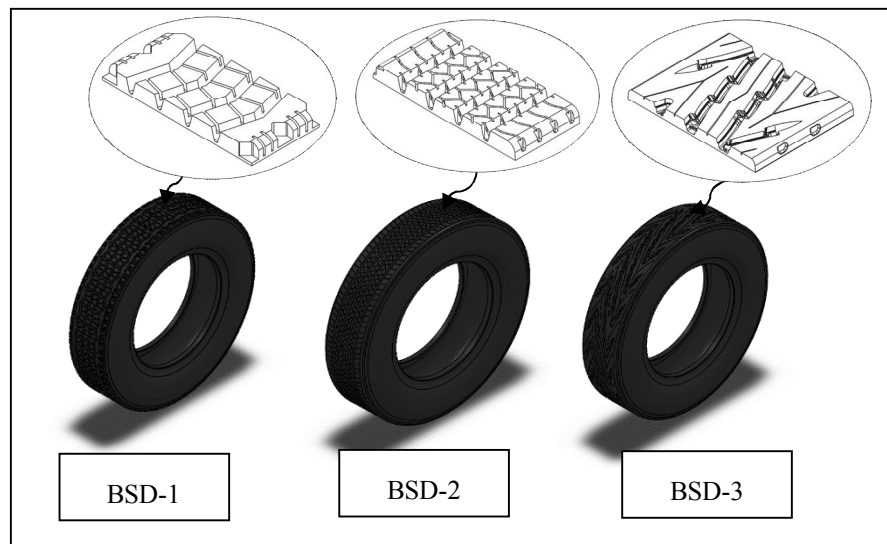


Figure 4. Retreaded truck tyre models for simulation

Material Model Development

Both the tread pattern and tyre casing can be modelled as a hyperelastic material whose constitutive model states that the stress-strain relationship for a non-linear elastic regime can be derived from a strain energy function. In this research, among various incompressible hyperelastic material models, the Mooney–Rivlin model [7], with two parameters whose strain energy function (W) is a linear combination of two invariants of the left Cauchy–Green deformation tensor [7], is selected as shown in (1):

$$W = C_{10}(I_1 - 3) + C_{01}(I_2 - 3), \quad (1)$$

where C_{10} and C_{01} are determined material constants, and I_1 and I_2 are the first and second invariants of the Green deformation tensor, defined in terms of the principal stretch ratios λ_1 , λ_2 and λ_3 as shown in (2) and (3):

$$I_1 = \lambda_1^2 + \lambda_2^2 + \lambda_3^2, \quad (2)$$

$$I_2 = \lambda_1^2\lambda_2^2 + \lambda_2^2\lambda_3^2 + \lambda_3^2\lambda_1^2. \quad (3)$$

Those material constants, as well as the material properties of a tyre ply and bead components defined as elastic plastic materials, are listed in Table 1. Tread pattern material properties have been established [17], while data on tyre casing, ply and bead properties were already provided [16].

Table 1. Material models of tyre components

Tyre component	Type of material model	Value
Tread pattern	Mooney-Rivlin	$C_{10} = 0.67$ MPa $C_{01} = 2.46$ MPa
Tyre casing	Mooney-Rivlin	$C_{10} = 0.51$ MPa $C_{01} = 1.86$ MPa
Ply	Elastic	$E^* = 3,050$ MPa $\mu^{**} = 0.33$
Bead	Elastic	$E = 95,000$ MPa $\mu = 0.33$

* Modulus of elasticity

** Poisson's ratio

Finite Element Model Development

In the preprocessing a finite element model by MSC.Patran software was created using geometry information shown in Figure 3 and material property data for each tyre component as obtained in Table 1. The element types of tetrahedron and hexahedron solid elements were selected for the tread pattern and tyre casing/ply/bead respectively for meshing as shown in Figure 5. Loading and boundary condition description and a schematic model with a testing drum for RR force determination based on ISO 28580-2009 regulation guideline are illustrated in Figure 6. The tyre tread is assumed to be a deformable body while the tyre rim and drum are rigid bodies. The contact types of tyre/drum components and surface interaction used in the model are shown in Table 2 with a selected friction coefficient of 0.50 [6]. There are three loading conditions: inflation

pressure of 0.79 MPa, loading force of 25.02 kN and drum rotating at 60 km/hr. In the solution phase a static analysis using MSC. Marc software was performed. In addition the simulated output variables, namely RR force, contact area and total strain energy, were found in the postprocessing of the finite element analysis.

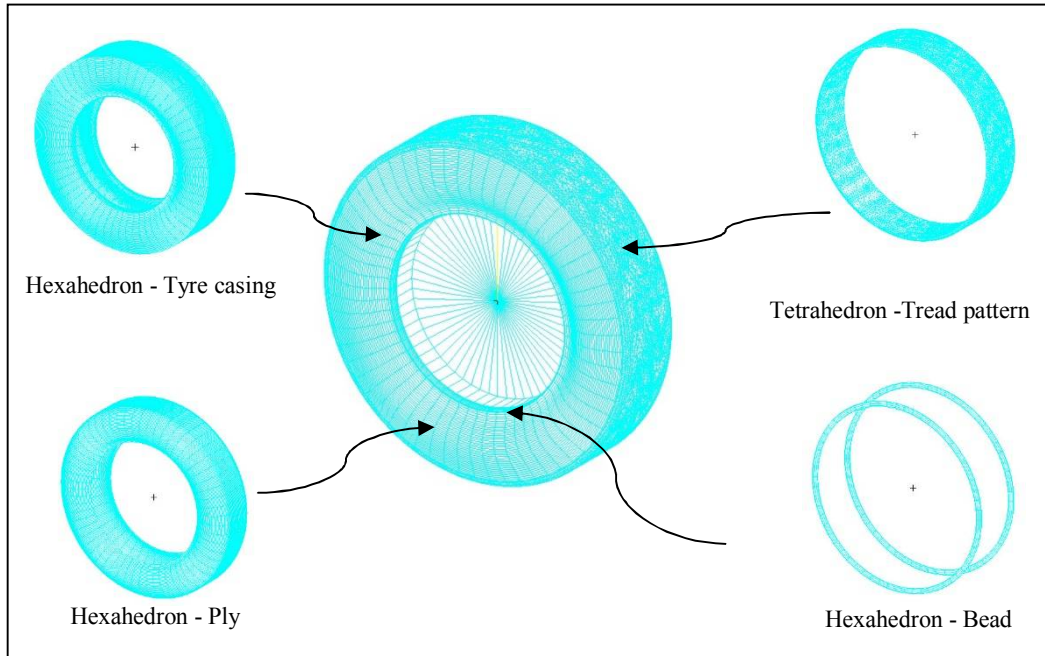


Figure 5. Finite element mesh for entire tyre components

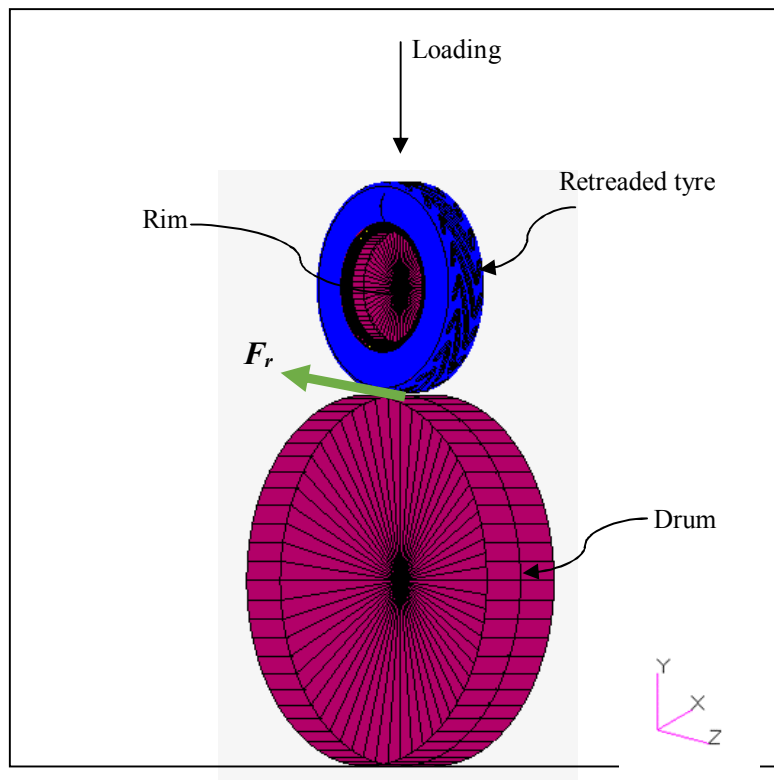


Figure 6. Schematic model with a testing drum and RR force, F_r , based on ISO 28580-2009 regulation guideline for RR force

Table 2. Contact types of tyre/drum components used in finite element model

Tyre/Drum component		Type of contact					
		Tread pattern	Tyre casing	Ply	Bead	Rim	Drum
Tyre	Drum						
Tread pattern	-	-	Glue	-	-	-	Touch
Tyre casing	-	Glue	-	Glue	Glue	Glue	-
Ply	-	-	Glue	-	-	-	-
Bead	-	-	Glue	-	-	-	-
Rim	-	-	Glue	-	-	-	-
-	Drum	Touch	-	-	-	-	-

EXPERIMENTAL WORK

The experimental work was conducted with three replications based on the power method specified in the ISO 28580-2009 guideline [6], which regulates methods in measuring RR force and its coefficient. Figure 7 shows a testing machine and a schematic experimental set-up to find RRCs using a tyre testing speed of 60 km/hr and a tyre inflation pressure of 0.79 MPa. In the ISO guideline the RRC can be found using formulas (4) (5) and (6):

$$RRC = \frac{F_r}{L_m} \quad (4)$$

where L_m is a preset loading of 25.02 kN specified in ISO 28580-2009 and F_r (N) is the RR force calculated by formula (5):

$$F_r = \frac{3.6V \times A}{U_n} - F_{pl} \quad (5)$$

in which V and A are input voltage and current respectively of the motor to drive a testing drum; U_n is the tyre testing speed and F_{pl} (N) is a parasitic loss when a load of 500 N is applied [6]:

$$F_{pl} = \frac{3.6V \times A}{U_n} \quad (6)$$

In this work experimental data for three tread patterns (Figure 8) of 10.00-20 pneumatic retreaded truck tyres were collected.

RESULTS AND DISCUSSION

Simulation Results

The simulated RR force (F_r) can be obtained from the contact force between the retreaded tyre and the drum in -z axis (Figure 6). For BSD-1, the simulated F_r and a preset loading (L_m) were found to be 178.14 N and 25.02 kN respectively. Thus, the RRC of BSD-1 can be calculated using formula (4) to be 7.12 kg/ton. Table 3 represents the simulated RR force and the resultant RRC for each tread pattern. In addition, contours of the simulated displacement for BSD-1, BSD-2 and BSD-3 are depicted in Figures 9-11. It is noted that the tyre deformations of 3.26, 4.36 and 2.63 mm in

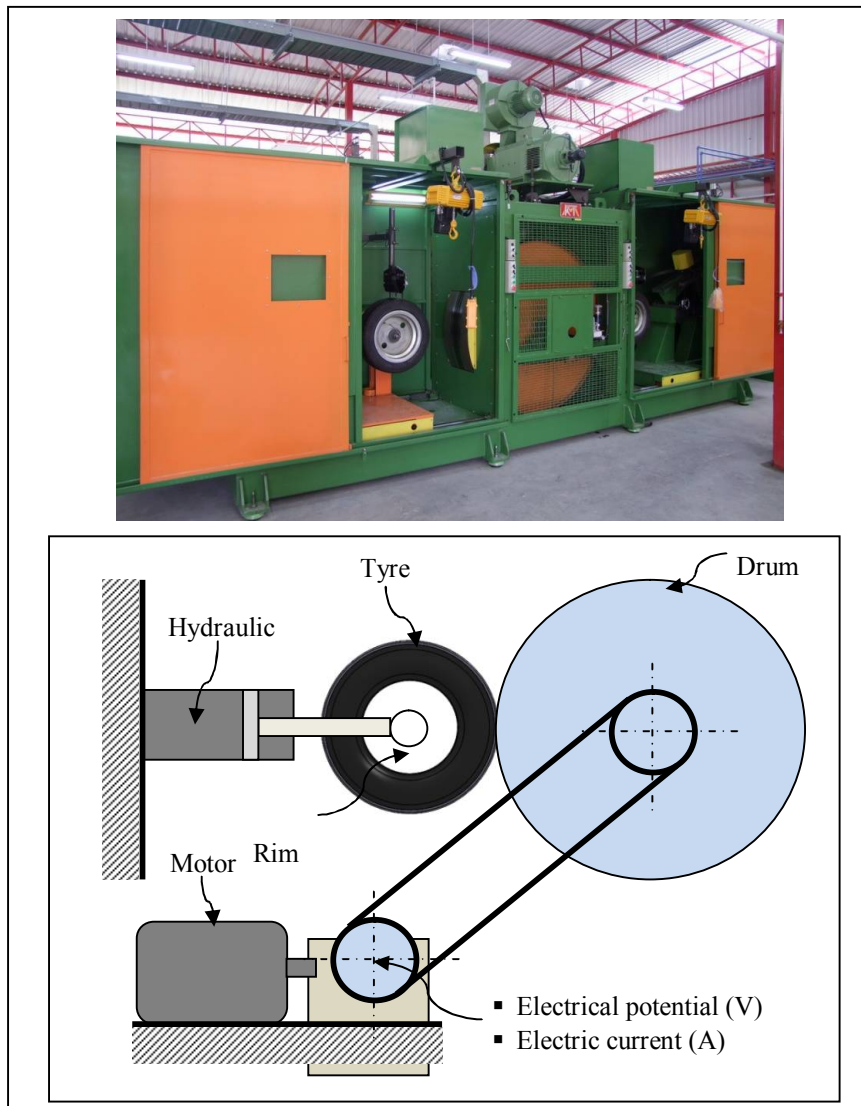


Figure 7. Drum tester for RR measurement (Kayton DTM-350 MS) and schematic experimental set-up for determination of RRC



Figure 8. Tyre tread patterns of the 20.00-10 biased pneumatic retreaded truck tyres

the y-direction for BSD-1, BSD-2 and BSD-3 respectively were found with a preset of 10-mm spacing between the tested tyre and the drum. It can be seen that the total vertical deformations were found to be 13.26, 14.36 and 12.63 mm respectively. In addition, the simulated total strain energies for BSD-1, BSD-2 and BSD-3 are shown in Figures 12-14. The maximum total strain energy of each tyre pattern was found to be 0.39, 0.47 and 0.43 MJ respectively. Furthermore, the simulated total strain energy rapidly rises from the tyre inflation to loading application and becomes stable in the drum rotation stage during incremental computation in the simulation, which is depicted in Figure 15.

Table 3. Simulated RR force and RRC for three tread patterns

Tread pattern	Rolling resistance force, F_r (N)	RRC (kg/ton)
BSD-1	178.14	7.12
BSD-2	183.15	7.32
BSD-3	168.38	6.73

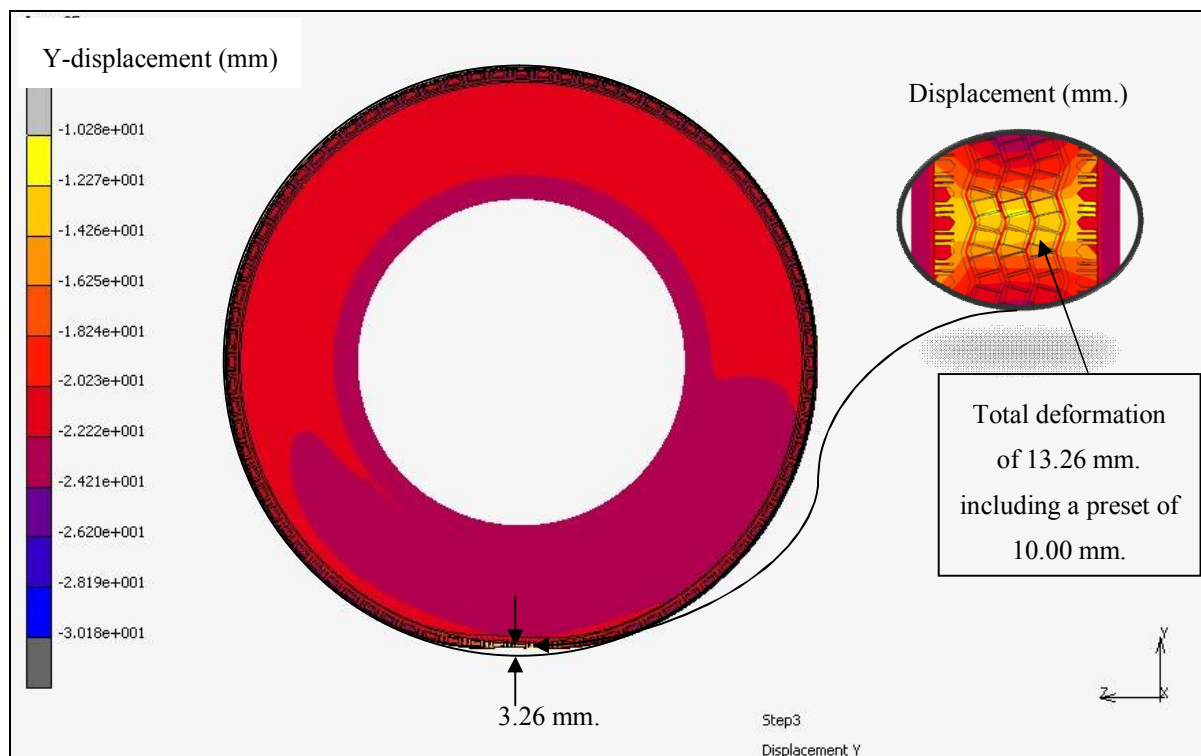


Figure 9. Simulated y-displacement contour of BSD-1

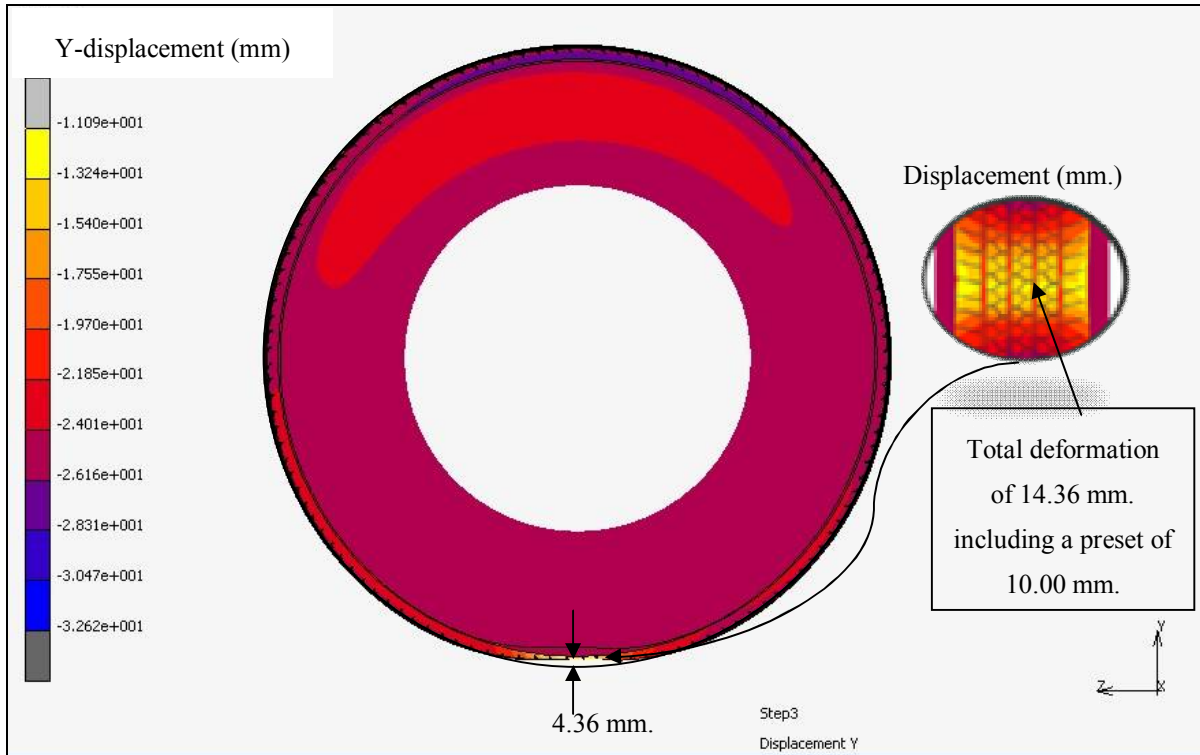


Figure 10. Simulated y-displacement contour of BSD-2

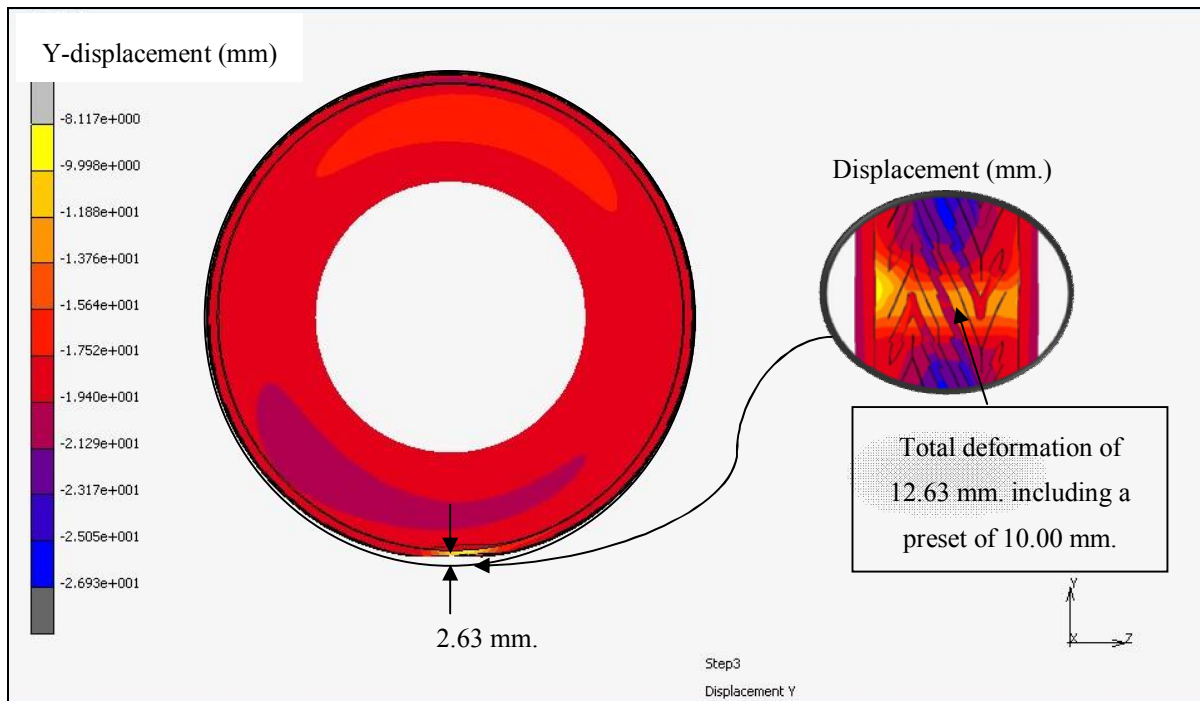


Figure 11. Simulated y-displacement contour of BSD-3

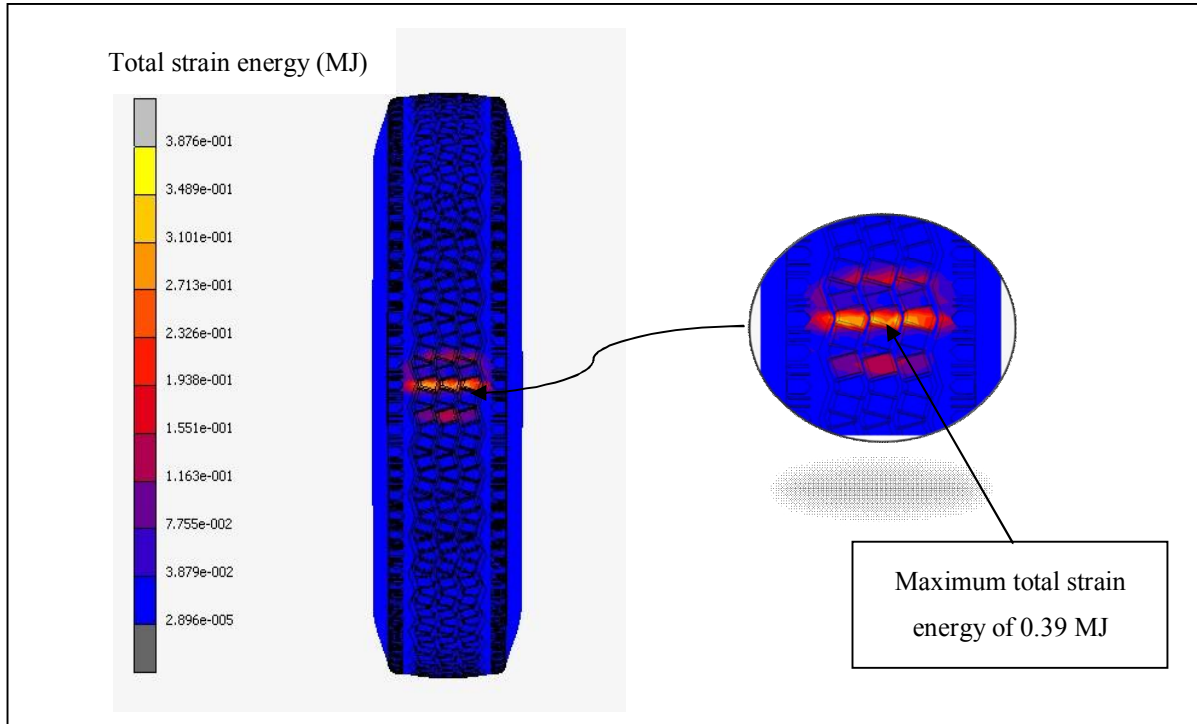


Figure 12. Simulated total strain energy contour of BSD-1

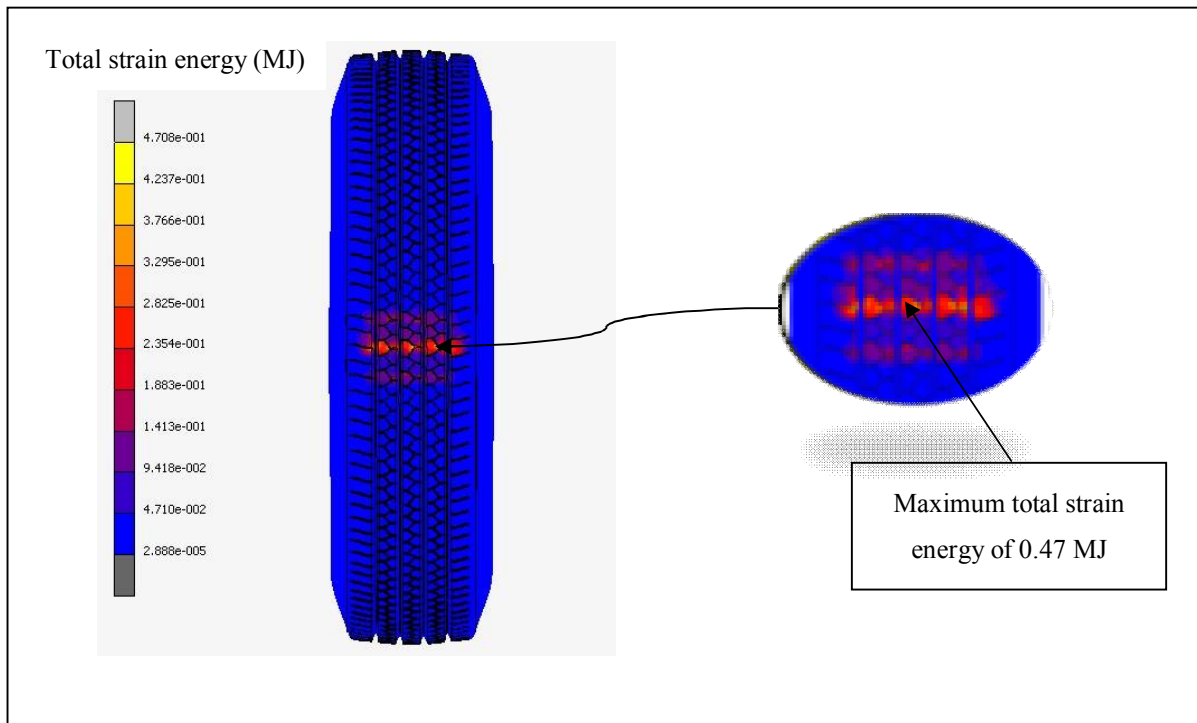


Figure 13. Simulated total strain energy contour of BSD-2

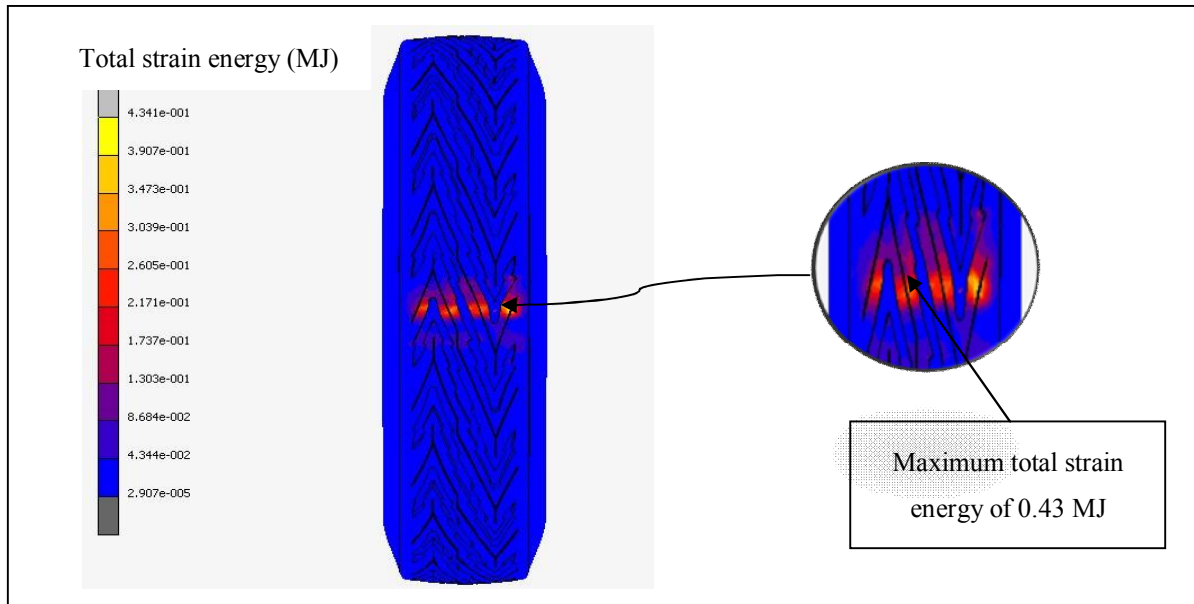


Figure 14. Simulated total strain energy contour of BSD-3

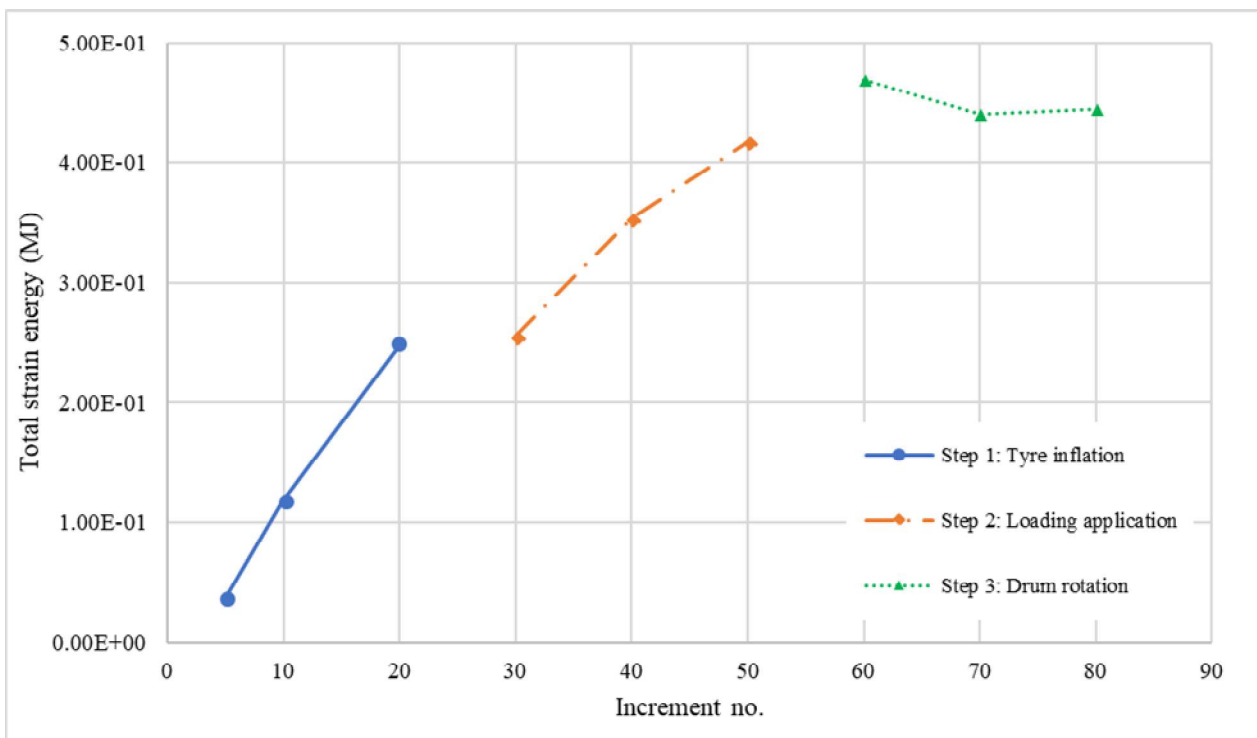


Figure 15. Simulated total strain energy variation during incremental analysis

Experimental Results and Comparison

Based on ISO 28580-2009, at a load of 500 N the measured input voltage and current for the motor driving the testing drum were 124 V and 12 A respectively, as shown in Table 4. Thus, the parasitic losses for all tyre tread patterns, according to formula (6), were 88.84 N. Additionally, the RR forces of BSD-1, BSD-2 and BSD-3, calculated using formula (5), were 197.01, 204.54 and 181.97 N respectively, at a load of 25.02 kN. Finally, both the experimental and simulated RRC

values for each tyre tread pattern, calculated using formula (4), are compared in Table 5. Differences between the simulated and experimental RRCs are at 9%, 10% and 7% for BSD-1, BSD-2 and BSD-3 respectively, which is acceptable. It can be seen that BSD-3 has the lowest experimental and simulated RRCs. It is thus notable that different tread patterns have a significant effect on the RRC value owing to different RR forces. Further investigation on this behaviour should be performed.

Table 4. Parasitic losses measurement and rolling resistance force measurement

Tread pattern	Parasitic losses measurement		Rolling resistance force measurement	
	Input voltage (V)	Electric current (A)	Input voltage (V)	Electric current (A)
BSD-1	124	12	126	38
BSD-2	124	12	126	39
BSD-3	124	12	126	36

Table 5. Comparison of RRCs for three tyre tread patterns

Tread pattern	Experimental RRC (kg/ton)	Simulated RRC (kg/ton)
BSD-1	7.87	7.12
BSD-2	8.17	7.32
BSD-3	7.27	6.73

CONCLUSIONS

A Numerical simulation and experimental verification of the RRC of the biased pneumatic retreaded truck tyres of size of 10.00-20 have been performed. The key output parameters such as RR force, total strain energy, as well as RRCs were analysed in this study. A good correlation between the simulated and experimental RRCs was found with a discrepancy range of 10% or lower. Consequently, the RRC prediction model can be further used for determining the effects of parameters, such as inflation pressure, load, speed and tread depth, on the RRC, which is related to fuel consumption efficiency in the near future.

ACKNOWLEDGEMENTS

The authors gratefully acknowledge the financial support through NSTDA-University-Industry Research Collaboration (NUI-RC) scholarship, Thailand's Ministry of Science and Technology, as well as the research funding from Energy Policy and Planning Office (EPPO), Thailand's Ministry of Energy. The authors also thank Bumrungrang Limited Partnership for its support and provision of retreaded tyres used in this work, as well as their contributions and valuable suggestions.

REFERENCES

1. S. Kohjiya and Y. Ikeda, "Chemistry, Manufacture and Applications of Natural Rubber", 1st Edn, Woodhead Publishing, Cambridge, **2014**, pp.325-351.

2. S. Dabic-Ostojic, M. Miljus, N. Bojovic, N. Glisovic and M. Milenkovic, "Applying a mathematical approach to improve the tire retreading process", *Resour.Conservat. Recycl.*, **2014**, 86, 107-117.
3. G. Ferrer, "The economics of tire remanufacturing", *Resour. Conservat. Recycl.*, **1997**, 19, 221-255.
4. W. Qiang and Q. Xiao-jie, "Study on the ground mechanical characteristics of load vehicles retreaded tires", Proceedings of International Conference on Materials for Renewable Energy and Environment, **2011**, Shanghai, China, pp.977-981.
5. Thai Industry Standards Institute, "TIS 2506-2553 : Precured tread for retreading of commercial vehicles tyres", **2010**, http://library.tisi.go.th/E/main_e.html (Accessed: November 2016).
6. International Organization for Standardization (ISO), "ISO 28580:2009 : Passenger car, truck and bus tyres – Methods of measuring rolling resistance - single point test and correlation of measurement results", **2009**, <https://www.iso.org/standard/44770.html> (Accessed: November 2016).
7. J. R. Cho, H. W. Lee, W. B. Jeong, K. M. Jeong and K. W. Kim, "Numerical estimation of rolling resistance and temperature distribution of 3-D periodic patterned tire", *Int. J. Solids Struct.*, **2013**, 50, 86-96.
8. S. Ghosh, R. A. Sengupta and G. Heinrich, "Investigations on rolling resistance of nanocomposite based passenger car radial tyre tread compounds using simulation technique", *Tire Sci. Technol.*, **2011**, 39, 210-222.
9. C. R. Bradley and A. Delaval, "On-road fuel consumption testing to determine the sensitivity coefficient relating changes in fuel consumption to changes in tire rolling resistance", *Tire Sci. Technol.*, **2013**, 41, 2-20.
10. T. Freudenmann, H.-J. Unrau and M. El-Haji, "Experimental determination of the effect of the surface curvature on rolling resistance measurements", *Tire Sci. Technol.*, **2009**, 37, 254-278.
11. J. R. Luchini, M. M. Motil and W. V. Mars, "Tread depth effects on tire rolling resistance", *Tire Sci. Technol.*, **2001**, 29, 134-154.
12. H. Taghavifar and A. Mardani, "Investigating the effect of velocity, inflation pressure, and vertical load on rolling resistance of a radial ply tire", *J. Terramechanics*, **2013**, 50, 99-106.
13. T. B. Rhyne and S. M. Cron, "A study on minimum rolling resistance", *Tire Sci. Technol.*, **2012**, 40, 220-233.
14. M. Gai-ling, X. Hong and C. Wen-yong, "Computation of rolling resistance caused by rubber hysteresis of truck radial tire", *J. Zhejiang Univ. Sci. A*, **2007**, 8, 778-785.
15. Z. Shida, M. Koishi, T. Kogure and K. Kabe, "A rolling resistance simulation of tires using static finite element analysis", *Tire Sci. Technol.*, **1999**, 27, 84-105.
16. S. Chae, "Nonlinear finite element modeling and analysis of a truck tire", *PhD Thesis*, **2006**, The Pennsylvania State University, USA.
17. S. Rodkwan and C. Daesa, "A Study on development of the truck retreaded tire based on natural rubber compounding for transportation efficiency improvement", Energy Policy and Planning Office Report, Ministry of Energy, Thailand, **2015**, Ch.4.